Exploring the S4 and S1 Prime Subsite Specificities in Caspase-3 with Aza-Peptide Epoxide Inhibitors[†,‡]

Rajkumar Ganesan,[§] Stjepan Jelakovic,[§] Amy J. Campbell,[||] Zhao Zhao Li,[||] Juliana L. Asgian,[||] James C. Powers,[||] and Markus G. Grütter*[,§]

Department of Biochemistry, University of Zurich, Winterthurerstrasse 190, CH-8057 Zurich, Switzerland, and School of Chemistry and Biochemistry, Georgia Institute of Technology, Atlanta, Georgia 30332-0400

Received February 21, 2006; Revised Manuscript Received May 24, 2006

ABSTRACT: Caspase-3 is a prototypic executioner caspase that plays a central role in apoptosis. Aza-peptide epoxides are a novel class of irreversible inhibitors that are highly specific for clan CD cysteine proteases. The five crystal structures of caspase-3−aza-peptide epoxide inhibitor complexes reported here reveal the structural basis for the mechanism of inhibition and the specificities at the S1′ and the S4 subsites. Unlike the clan CA cysteine proteases, the catalytic histidine in caspase-3 plays a critical role during protonation and subsequent ring opening of the epoxide moiety and facilitates the nucleophilic attack by the active site cysteine. The nucleophilic attack takes place on the C3 carbon atom of the epoxide and results in an irreversible alkylation of the active site cysteine residue. A favorable network of hydrogen bonds involving the oxyanion hole, catalytic histidine, and the atoms in the prime site of the inhibitor enhance the binding affinity and specificity of the aza-peptide epoxide inhibitors toward caspase-3. The studies also reveal that subtle movements of the *N*-terminal loop of the β-subunit occur when the P4 Asp is replaced by a P4 Ile, whereas the *N*-terminal loop and the safety catch Asp179 are completely disordered when the P4 Asp is replaced by P4 Cbz group.

Caspases are a family of cysteine aspartate specific proteases that have essential functions in apoptosis and cytokine activation (*1*, *2*). On the basis of their biological functions, they are classified as initiators (caspase-8, -9, and -2) and executioners (caspase-3, -6 and -7). Caspase-3 is the most abundant caspase in vivo (*3*−*5*), and it is the best characterized family member. Apart from its established role as a prototypic executioner caspase, several nonapoptotic roles of caspase-3 are emerging (*6*−*8*). Currently, many industrial and academic laboratories are engaged in the design of specific inhibitors for caspase-3 to regulate its activity for the therapeutic intervention of diseases, such as myocardial infarction, Alzheimer's, stroke, Parkinson's, sepsis, and Huntington's disease (*9*). Even though the executioner caspases-3 and -7 share high sequence similarity and substrate specificity, they have distinct roles in apoptosis (*10*). Thus specific inhibitors for caspases would assist in deciphering the precise role of each caspase in the execution phase of apoptosis. Caspases demonstrate stringent specificity for an aspartic acid residue in P1 position of a substrate. Within the caspase family, substrate selectivity is highest for the P4 residue (*11*). Apart from P4, the prime site could also be utilized to gain specificity among caspases. Although considerable effort has been devoted to the optimization of the interactions of caspase inhibitors in the S1−S4 subsites (*9*, *12*), only a few studies exist that analyze the interactions of substrates or inhibitors at the prime site (*13*−*16*).

Initial studies using fluorescent peptidyl substrates indicated a preference for small residues (Gly, Ala, Ser) at position P1′ for caspase-1, -3, -6, and -8. A few peptidomimetic compounds that bind to the prime site were identified for caspase-3 and were characterized structurally (*13*). The halogen methyl ketones and aldehydes are the most commonly used electrophilic groups (warheads), which were coupled with the preferred tetra/penta peptide recognition sequence of caspases (*9*). Because these warheads are highly reactive and tend to inhibit other clan CA cysteine proteases (*17*−*20*), the search for potential warheads that are highly selective for caspases becomes increasingly important. To overcome the problem of a lack of selectivity, we have recently reported the identification and characterization of aza-peptide epoxide and Michael acceptors as a new class of irreversible caspase inhibitors that are highly specific for clan CD cysteine proteases (*21*−*23*). In this article, we report the crystal structures of caspase-3 in complex with five of the aza-peptide epoxides inhibitors, containing modifications at the P1′ and P4 positions, to understand the specificity, binding mode, and the mechanism of inhibition in these regions of the active site. The modifications at the prime site were intended to gain selectivity for caspase-3, whereas the study with a tripeptide (-EVD-) derivative and a tetra-

[†] The financial support from the Swiss National Science Foundation (6M3100A-1022181) and Baugartenstiftung (Zürich, Switzerland) and from the National Institute of General Medical Sciences (GM61964) is gratefully acknowledged.

[‡] The atomic coordinates and structure factures for caspase-3 aza-peptide epoxide inhibitor complexes have been deposited with the Protein Data Bank, and the accession codes are 2CDR, 2CNK, 2CNL, 2CNO, and 2CNN.

* Corresponding author. Tel: +41 (44) 635 5580. Fax: +41 (44) 635 6834. E-mail: gruetter@bioc.unizh.ch.

[§] University of Zurich.

[||] Georgia Institute of Technology.

10.1021/bi060364p CCC: $33.50
Published on Web 07/07/2006

peptide (-IETD-) derivative, was aimed at understanding the influence of the P4−residue interaction and ordering of the *N*-terminal loop of the β-subunit. The C2 carbon atom of the epoxide moiety binds covalently to the thiol group of the active site cysteine of caspase-3. This observation is in contrast to the previous proposal where the covalent bond was reported to occur between the C2 carbon atom of the epoxide inhibitor and the thiol group of active site cysteine in caspase-1 (*23*).

EXPERIMENTAL PROCEDURES

Materials and Methods

Caspase Purification. Human recombinant caspase-3 was produced in *Escherichia coli* as inclusion bodies, refolded, and purified. Briefly, the cloned genes for the α-subunit (Met-Ser_{29}-Asp_{175}) and the β-subunit (Met-Ala-Ser_{176}-His_{277}) were inserted in the *Nco*I/*Bam*HI sites of the pET11d plasmids (Novagen). For the separate expression of both subunits, *Escherichia coli* BL21-CodonPlus (DE3)-RIL cells (Stratagene) containing one of the two plasmids were grown to a density of $A_{600} = 0.5$ at 37 °C in a 0.5-L Luria−Bertani medium. Expression was induced by the addition of IPTG (1 mM), and the culture was shaken at 37 °C for 4 h post-induction. Cells were harvested, washed in PBS buffer, and lyzed using a French press. Because of overexpression, the protein was localized in the inclusion body portion. Refolding was achieved by the rapid mixing of equimolar amounts of each subunit to a final concentration of about 100 μg of subunit/L in the refolding buffer (100 mM HEPES at pH 7.5, 10% sucrose, 1% CHAPS, 100 mM NaCl, and 10 mM DTT) and was incubated overnight at room temperature with continuous stirring. Misfolded and aggregated proteins were removed by centrifugation (5000*g*, 30 min), and the supernatant was concentrated using an Amicon-stirred cell. To reduce the salt concentration and to facilitate binding to an anion exchange column (Resource-Q, GE Healthcare), the protein solution was dialyzed against the anion exchange buffer (20 mM Tris at pH 8.0, 30 mM NaCl and 10 mM DTT) prior to chromatography. The protein was eluted using a 300 mM NaCl gradient. The pure and active caspase-3 was further purified by size exclusion chromatography (Superdex S200, GE Healthcare) with a buffer containing 20 mM Tris at pH 8.0, 50 mM NaCl, and 10 mM DTT. The fractions containing pure and active caspase were pooled and concentrated by ultrafiltration to a final concentration of 10 mg/mL, and the final yield was about 5−7 mg/L of culture. The purified caspase was subsequently inhibited with a 3-fold molar excess of the inhibitor.

Crystallization and Data Collection. Cocrystals of the complex between recombinant human caspase-3 and aza-peptide epoxide inhibitors were grown from 2 to 4 μL of hanging drops formed by mixing equal volumes of protein (10 mg/mL in 20 mM Tris/HCl at pH 8.0 and 10 mM DTT) and the reservoir solution. The reservoir solution consisted of 15% (w/v) poly(ethylene glycol) 6000 and 100 mM sodium citrate at pH 5.0. Crystals ($\sim 300 \times 200 \times 100\ \mu m^3$) grew within 2−3 days. For data collection, the crystals were frozen in a nitrogen stream after a short soak in the reservoir solution containing 20% glycerol. The crystals belong to the space group *I*222, and the typical unit cell dimensions were $a = 67.2$, $b = 83.3$, and $c = 96.0$ Å. Diffraction data for inhibitors **1**, **2**, **3**, and **5** were collected using a rotating anode generator (Bruker-Nonius, FR591) at 100 K. Images were integrated with MOSFLM (*24*) and scaled with SCALA (*25*) from the CCP4 suite of programs. Diffraction data for inhibitor **4** were collected at the Swiss Light Source synchrotron (Paul Scherrer Institute, Villigen, Switzerland). Data processing was done with the program XDS (*26*).

Structure Solution and Refinement. The structure was solved by the difference Fourier technique. Structure refinement and automated water addition were performed using the program CNS (*27*), and model building was done with the program O (*28*). Iterative cycles of refinement and model building were performed. To simplify the dictionary of restraints for aza-peptide epoxide inhibitors, the molecule was treated as three parts, the *N*-terminal blocking group (Cbz), tripeptide portion (DEV), and the P1−Asp[1] along with P1′ peptidomimetic. The final crystallographic *R* and free *R* factors were in the range of 16−19% and 19−22%, respectively. The final model consisted of residues 29−174 of the α-subunit and 176−277 of the β-subunit in the case of **1**, **2**, **3**, and **5**, and the residues 176−185 of the β-subunit were disordered in case **4**. A summary of the crystallographic data processing and refinement statistics for the caspase-3−aza-peptide epoxide inhibitor complexes are given in Tables 1 and 2, respectively.

RESULTS

Inhibitor Design. Inhibitor potency critically depends on the structure of the peptide moiety and the chemical reactivity of the warheads. Inhibitors such as E-64 and their synthetic analogues containing an epoxysuccinyl moiety as the warhead are specific inhibitors for clan CA cysteine proteases (*29*). Epoxysuccinyl dipeptides without an aspartic acid residue do not inhibit caspase-1 (*30*), and a variety of epoxysuccinyl peptides containing aspartate do not inhibit other caspases (Powers, J. C., and Özlem Dogan Ekici, unpublished results). The reason for the inertness of the E-64 derivatives against caspases might be the unparalleled selectivity for an aspartic acid residue in the S1 subsite or the location of the warhead. The design strategy for the inhibitors presented here was to place an epoxide group at the *C*-terminus of a P1 aza aspartate and also to retain an additional carbonyl group at the prime site by using the epoxysuccinyl moiety (Figure 1).

Structure-Based Mechanism of Inhibition. Epoxides are weak electrophiles, but they tend to become highly electrophilic upon protonation. Protonation is critical for the ring opening and subsequent alkylation of the active site thiol group of Cys_{163}. When the epoxides are flanked by carbonyl groups on either side, they are preactivated and referred to as epoxysuccinyl inhibitors. This strategy has led to the identification of compounds that are potent inhibitors of caspases (*21*, *23*). These inhibitors possess a dual advantage as a result of the combination of the high reactivity of the activated epoxides coupled with enhanced binding properties of regular substrate-like peptides.

In general, the inactivation of cysteine proteases by epoxide inhibitors proceeds through the nucleophilic attack

[1] Abbreviations: AAsp, Aza-aspartic acid; AMC, 7-amino-4-methyl coumarin; LBHB, low-barrier hydrogen bond; Z/Cbz, benzyloxycarbonyl; E-64, L-*trans*-epoxysuccinyl-leucylamide-(4-guanidino)-butane.

Table 1: X-ray Data Collection Statistics of Caspase-3/Aza-Peptide Epoxide Complex Crystals[a]

	1	**2**	**3**	**4**	**5**
	caspase-3/ Cbz-DEVaD -(*S*,*S*) EP-CO-N $(CH_2Ph)_2$	caspase-3/ Cbz-DEVaD -(*S*,*S*) EP-COO $-CH_2Ph$	caspase-3/ Cbz-DEVaD -(*S*,*S*) EP-CO-NH $-CH_2Ph$	caspase−3/ Cbz-EVaD -(*S*,*S*) EP-CO-NH $-Ch_2CH_2Ph$	caspase-3/ Cbz-LETaD -(*S*,*S*) EP-CO-Ala $-NHCH_2$ Ph
space group	*I*222				
unit cell dimensions (Å)	*a* = 65.9 *b* = 83.4 *c* = 96.4	*a* = 66.8 *b* = 83.8 *c* = 96.5	*a* = 67.7 *b* = 84.0 *c* = 96.2	*a* = 69.1 *b* = 83.5 *c* = 95.8	*a* = 67.9 *b* = 83.7 *c* = 96.2
resolution range (Å)	20.0−1.70 (1.79−1.70)	20.0−1.75 (1.84−1.75)	20.0−1.67 (1.76−1.67)	20.0−2.05 (2.15−2.05)	20.0−1.69 (1.78−1.69)
unique reflections	28860 (3974)	27485 (3983)	31449 (4313)	16966 (2257)	30129 (3591)
redundancy	4.1 (3.8)	3.8 (3.6)	4.4 (4.3)	4.5 (5.9)	4.6 (4.3)
R_{merge} (%)	4.8 (29.9)	5.6 (24.6)	6.4 (32.6)	2.5 (3.6)	6.6 (28.1)
completeness (%)	97.7 (93.0)	99.7 (100)	98.1(93.4)	95.4 (97.7)	97.8 (85.5)
average I/σ	18.8 (3.9)	17.0 (5.5)	17.3(3.8)	31.9 (25.3)	19.3 (4.3)

[a] The values in parentheses refer to that of the highest resolution shell.

Table 2: Refinement Statistics of Caspase-3/Aza-Peptide Epoxide Crystal Structures

	1	**2**	**3**	**4**	**5**
	caspase-3/ Cbz-DEVaD -(*S*,*S*) EP-CO-N $(CH_2Ph)_2$	caspase-3/ Cbz-DEVaD -(*S*,*S*) EP-COO $-CH_2Ph$	caspase-3/ Cbz-DEVaD -(*S*,*S*) EP-CO-NH $-CH_2Ph$	caspase−3/ Cbz-EVaD -(*S*,*S*) EP-CO-NH $-Ch_2CH_2Ph$	caspase-3/ Cbz-LETaD -(*S*,*S*) EP-CO-Ala $-NHCH_2$ Ph
resolution (Å)	20.0−1.70	20.0−1.75	20.0−1.67	20.0−2.05	20.0−1.69
R	17.4	16.2	18.5	16.4	18.0
R_{free}	20.1	18.9	21.4	19.4	20.4
			Number of atoms		
protein	2004	1996	2004	1931	1996
ligand	62	55	55	48	60
water	363	403	361	299	348
			Average B-factors		
protein(Å^2)	18.2	13.1	18.8	14.2	16.9
ligand (Å^2)	31.6	22.5	30	41.0	35.6
water (Å^2)	38	34.3	37.7	31.1	36.0

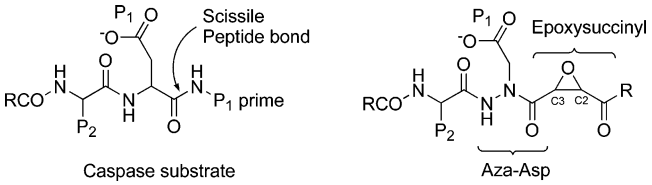

FIGURE 1: Design of aza-peptide epoxide inhibitors based on the structure of caspase substrates. Selectivity was achieved by the introduction of an epoxide moiety at the *C*-terminus of the P1-aza aspartic acid residue.

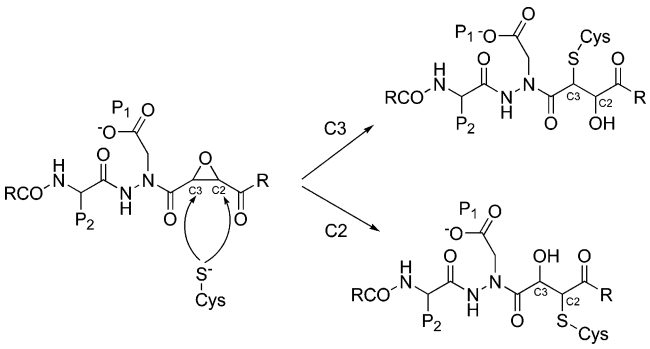

FIGURE 2: Two possible pathways for the mechanism of inhibition of caspase by aza-peptide epoxides involving either a C2 attack or a C3 attack resulting in the epoxide ring opening and formation of a thioether adduct.

of the active site thiol group on either the C2 or C3 carbon atom of the oxirane ring. This irreversible thioalkylation could follow two different pathways (Figure 2). In a previous study, it was proposed that the nucleophilic active site thiol group of caspase-1 reacts on the C2 carbon atom of an aza-peptide epoxide inhibitor (*23*). In contrast, the high resolution crystal structures of caspase-3 complexes presented here clearly demonstrate that the nucleophilic attack is on the *re* face of the C3 carbon atom, creating a covalent thioether bond (typically C−S$^\gamma$ = 1.8 Å) between the C3 carbon and the sulfur atom of the active site cysteine (Cys_{163}) (Figure 3a). Aza-peptides with good leaving groups will inhibit both serine and cysteine proteases with the formation of stable acyl enzyme derivatives (*30*, *31*). The acyl enzyme complexes formed by the reaction of aza-peptides with cysteine proteases are thiocarbamates and are generally more stable than the thioesters formed from normal peptide substrates. The reason is the inability of a water molecule to nucleophilically attack the thiocarbamyl group of the acyl enyzme

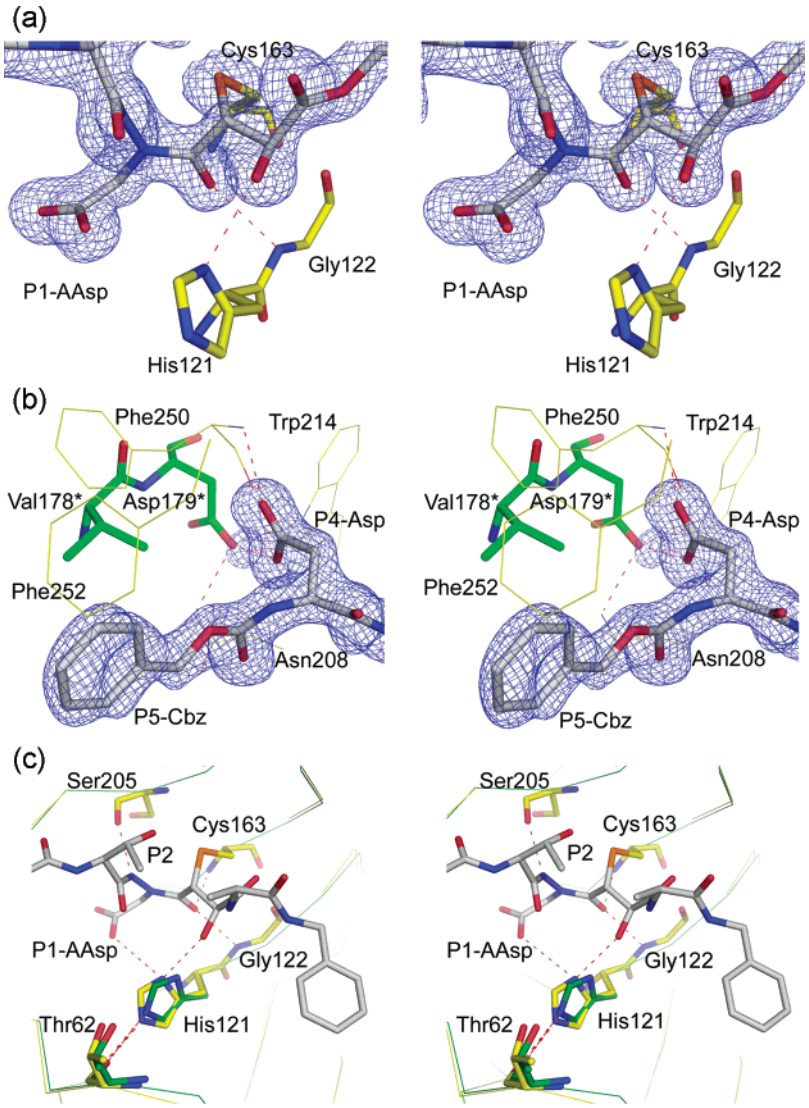

FIGURE 3: Close-up view of the active site of caspase-3. (a) The nucleophilic attack resulted in the formation of a covalent bond between S^{γ} and C3, and the stereochemistry of the enzyme inhibitor **2** adduct underwent an inversion in configuration from *2S,3S* to *2R,3R*. The prominent hydrogen bond interactions include the P1 carbonyl with the oxyanion hole and the catalytic His_{121} with the prime site hydroxyl group (C2 carbon) (Figure 4a−e). (b) A low barrier hydrogen bond (bond length 2.4 Å) is observed between the P4 Asp of inhibitor **2** and the safety catch Asp_{179} from the *N*-terminal loop of the β-subunit. (c) The superposition of the active site residues of caspase-3 in complex with compound **5** and the Ac-DEVD−CHO complex (green, pdb code: 1PAU). The catalytic His_{121} of compound **5** complex is rotated approximately 15° about its $\chi 1$ and $\chi 2$ angles, resulting in a hydrogen bond formation with P1 Asp while retaining its interaction with Thr_{62}. The electron density map was contoured at 1.0 σ, and the hydrogen bond interactions are drawn as red dashed lines. The residues belonging to the other monomer are indicated by an asterisk.

complex (*32*). The increased stability of thiocarbamates is a consequence of the unique conformational and electronic properties of the aza-amino acid residue containing an α-nitrogen atom.

As a consequence of the nucleophilic attack by the active site thiolate following an S_N2 reaction mechanism, the stereochemistry of the enzyme inhibitor adduct undergoes an inversion in configuration. The configuration changes from *2S,3S to 2R,3R* (Figure 3a). The change at the C2 carbon atom is due to the nucleophilic attack, whereas the change at the C3 carbon atom is due to the alteration in the ranking order of the substituents. The high resolution and well-defined electron density map allowed us to make an unambiguous interpretation of the chiralities at the C2 and C3 atoms. The stereochemical changes observed in our structural studies are similar to those observed in other cysteine protease−epoxysuccinyl inhibitor complexes (*29*, *31*, *33*).

In the case of clan CA cysteine proteases, the critical protonation event of the epoxide ring is driven by water molecules (*34*). The enzyme−inhibitor structures with compounds (**1**−**5**) show that the nascent hydroxyl group formed as a result of the epoxide ring opening is oriented toward the active site His_{121}, forming a hydrogen bond (hydrogen bond distance ranging from 2.7 to 2.9 Å) (Figure 4). This strongly indicates that in caspases (or at least caspase-3), unlike in clan CA cysteine proteases, the catalytic His_{121} plays a key role in the protonation and subsequent ring opening of the epoxide ring.

Structure and Binding Mode of Caspase-3: Aza-Peptide Epoxide Inhibitors. We have determined five crystal structures of caspase-3−aza-peptide epoxide inhibitor complexes.

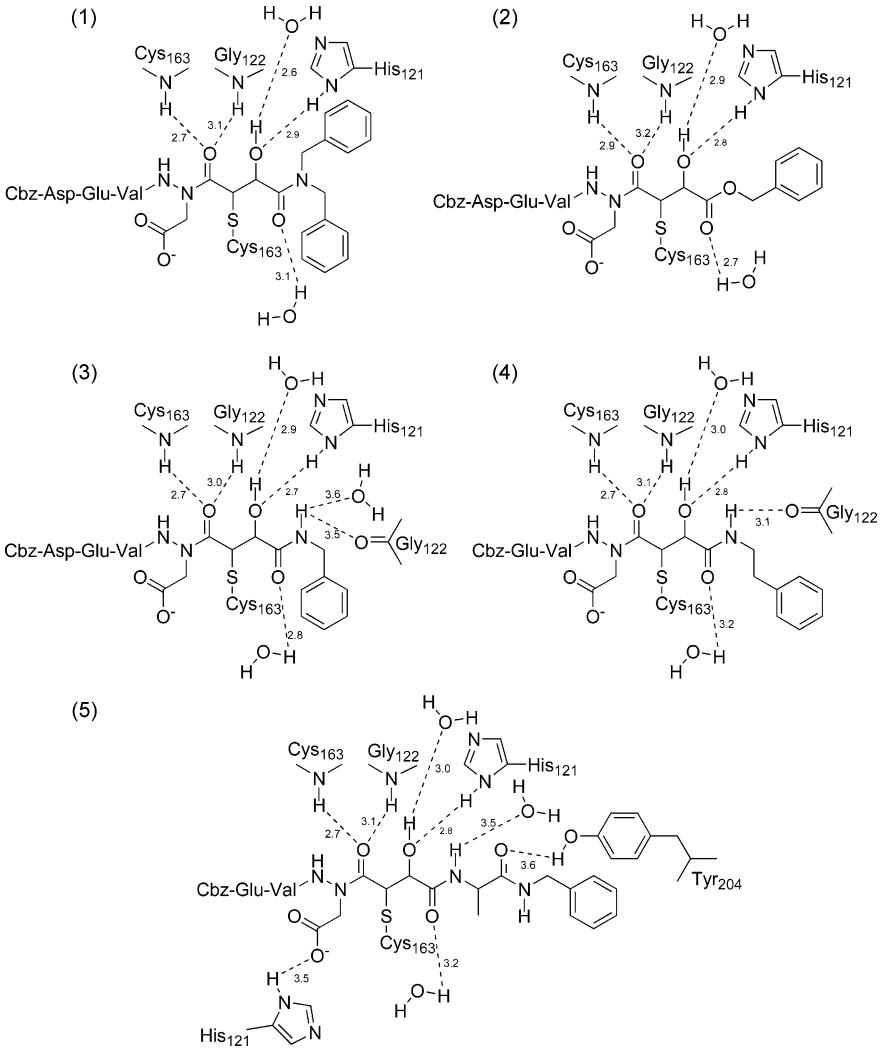

FIGURE 4: Chemical structures and hydrogen bond networks at the prime site for caspase-3 in complex with aza-peptide inhibitors **1**−**5**. The nascent hydroxyl group at the C2 carbon atom formed as a result of nucleophilic attack is involved in a hydrogen bond formation with catalytic His_{121}. The P1-carbonyl group is stabilized with hydrogen bond interaction of the oxyanion hole, whereas the P1 prime carbonyl group is stabilized with a conserved water molecule. The interaction between the P1 Asp and His_{121} in the case of the structure of caspase-3 in complex with compound **5** implies, apart from its implications in catalysis, that His_{121} plays a role in substrate binding.

The interactions of the P1−P4 moieties of the aza-peptide epoxide inhibitors in the substrate binding cleft of caspase-3 are similar to those observed for peptidyl aldehyde or halogen methyl ketone inhibitors (*35*, *36*), thus closely mimicking substrate-like binding. The inhibitors used for the structural studies were all trans (*2S,3S*) stereoisomers. The tetrapeptide (-DEVD-)-based inhibitors are the *N*,*N*-dibenzyl amide derivative **1**, the *N*-benzyl amide derivative **2**, and the benzyl ester derivative **3**. The tripeptide (-EVD-)-based inhibitor is a *N*-phenethyl amide derivative **4**, and compound **5** is a tetrapeptide (-IETD-)-based inhibitor containing an alanine residue blocked by a *N*-benzyloxycarbonyl group at the *C*-terminus. The chemical structures, along with the key hydrogen bond interactions in the prime site of the caspase-3−aza-peptide epoxide inhibitor complexes, are illustrated in Figure 4a−e. A hydrogen bond between the prime site carbonyl group and a water molecule is conserved in all the complexes (Figure 4).

The overall structure of the enzyme in the complexes analyzed here is similar to other known crystal structures of caspase-3 (*35*, *36*). The α- and *β*-subunits fold into a central six-stranded mixed *β*-sheet that is flanked on both sides by 5 α-helices. This architecture, which is designated as the caspase hemoglobinase fold, is conserved throughout all caspase structures. Superposition of the C^{α} atoms of different caspase-3 inhibitor complexes resulted in a root-mean-square deviation of 0.3 Å (*35*, *36*). This indicates that large scale conformational changes do not occur upon binding of the prime site substituents. However, rearrangements occur in residues that directly interact with the inhibitor. The geometries of the epoxide inhibitors bound to caspase-3 were well defined in the electron density maps, allowing an unambiguous interpretation of the atoms of the inhibitor located in the prime site (Figure 3a).

Influence of Inhibitor Structure on Binding and Rate of Inactivation. Aza-peptides are analogues of peptides in which the α-CH group is exchanged by a nitrogen atom (*37*−*39*). This substitution has a profound effect on the reactivity and results in the loss of the chiral center. The presence of the free electron pair on the aza-nitrogen atom leads to an extension of the area of planarity in comparison to a normal peptide linkage (*40*). The additional limitation of free rotation seems to allow the side chains to adopt a configuration that is between the D and L configuration (*37*, *38*). Consequently,

there is an increase in acidity of the NH group attached to the aza-nitrogen atom, which strengthens the P1-amide hydrogen bond to the backbone carbonyl group of Ser_{205} (Figure 3c). The importance of the backbone intermolecular hydrogen bond interaction was studied previously (*41*). A dramatic decrease in potency was observed for caspase-1 when the P1-amide proton was replaced by a methyl group underscoring the significance of this interaction for binding and potency. In the current structures, the inhibitor moiety extends along the primed and nonprimed subsites of the enzyme, and it is stabilized by a series of hydrogen bonds and hydrophobic interactions (Figure 4).

Interactions at the Prime Site of Caspase-3. The structural and chemical properties of the prime site region of caspase-3 indicate a preference to bind hydrophobic moieties of an inhibitor. Inhibitors containing such prime site residues might bind with higher affinity and would offer higher selectivity for caspase-3. The prime site in caspase-3 is predominantly hydrophobic and is delineated by four loop regions: the 179-loop (between strand β1 and helix α2), the 240-loop (between strand β3 and helix α3), the *C*-terminal loop from the α subunit, and by a loop (between helix α3 and strand β4) from the β subunit. The interactions of the P2 and P3 residues of the inhibitor are similar to the ones reported in other caspase-3 structures (*35*, *36*). In all crystal structures reported here, the P1 carbonyl group, which is a part of the aza-aspartic acid, extends toward the oxyanion hole and is stabilized by hydrogen bonds to the backbone amide nitrogens of Gly_{122} and Cys_{163} (Figure 4). These interactions are similar to those observed in the crystal structures of caspases in complex with halo methyl ketones (*35*, *42*). These interactions contribute to the stabilization of the enzyme inhibitor complex and also help to ideally orient the inhibitor for the subsequent nucleophilic attack by the active site Cys_{163} S^{γ} atom. A unique feature of all crystal structures of caspase-3 aza-peptide epoxide complexes is the rotation of the catalytic His_{121} around C1 and C2 by approximately 15°. During this rotation, the hydrogen bond between the His_{121} N^{ϵ} atom and the backbone carbonyl of Thr_{62} (putative third residue of the catalytic triad) stays intact because the geometry of this hydrogen bond is nearly collinear with the $C^{\alpha}-C^{\beta}$ bond (Figure 3c). The movement of His_{121} is required because otherwise, a steric clash with the newly formed hydroxyl group at the C2 carbon atom would occur. This movement results in the formation of a hydrogen bond with the P1 Asp residue in the case of the structure of caspase-3 in complex with **5**. The interaction between the catalytic His_{121} and P1 Asp implies that His_{121}, apart from its implications in catalysis, plays a role in substrate binding.

Inhibitor **1** is the most potent inhibitor used in this structural study. It possesses a bulky dibenzyl moiety that best fits the large cavity in the prime site and effectively buries altogether about 740 Å^2 of the enzyme accessible surface on binding. The order of reactivity correlates well with the calculated buried surface area upon the binding of the inhibitor (Table 3). While one of the phenyl rings is involved in hydrophobic interaction with Tyr_{204}, Thr_{166}, and Glu_{123}, the other phenyl ring fits the hydrophobic pocket formed by Met_{61} and Phe_{128} of the prime site (Figure 5a). The monobenzyl derivative **3**, unlike its dibenzyl counterpart, has a proton donating amide group and forms a hydrogen bond with the backbone carbonyl group of Gly_{122}. Despite this additional hydrogen bond, the absence of the second phenyl ring resulted in a 50% decrease in the observed k_2 value (Table 3). Moreover, the phenyl ring is not placed ideally in the hydrophobic pocket; rather, it is oriented in an unfavorable position toward the carboxyl group of Glu_{123} (Figure 5a). A superposition of the benzyl ester derivative **2** with **1** shows, that its phenyl ring occupies the same pocket as one of the phenyl rings of compound **1**. Compound **2** is as potent as compound **1** as it effectively buries the residues Tyr_{204}, Thr_{166}, and Glu_{123} delineating this pocket (Figure 5a). The decreased affinity for compounds **4** and **5** is predominantly due to the nonoptimal residues in the P4 position. In addition, the extension of the aliphatic chain by one carbon in compound **4** does not seem to improve the affinity in the prime site. The terminal phenyl ring is very flexible because it is destabilized because of the presence of a charged side chain of Glu_{123}. However, the presence of an alanine residue in the prime site in the case of compound **5** appears to be favorable because its methyl group is stabilized by the side chain of P2 threonine residue (Figure 5b).

Table 3: Second Order Inactivation Rate Constants (k_2) and Buried Surface Area for Aza-Peptide Epoxide Inhibitors against Caspase-3

	aza-peptide epoxide inhibitors[a]	k_2 (M^{-1} s^{-1})[b]	buried accessible surface area (Å^2)
1	Cbz-DEVaD-(*S*,*S*) EP-CO-N(CH_2Ph)2	2170000	742
2	Cbz-DEVaD-(*S*,*S*) EP-COO-CH_2Ph	1910000	682
3	Cbz-DEVaD-(*S*,*S*) EP-CO-NHCH_2Ph	1090000	619
4	Cbz-EVaD-(*S*,*S*) EP-CO-NH-CH_2CH_2Ph	27300	614
5	Cbz-LETaD-(*S*,*S*) EP-CO-Ala-NH-CH_2Ph	1280	618

[a] The aza-aspartic acid residue is represented by aD. [b] The k_2 values were compiled from ref 23 (*23*).

Specificity of Caspase-3 in the S4 Pocket. Caspase-3 and caspase-7 are highly selective for an aspartic acid as the P4 residue (*11*). In the case of caspase-3, the affinity for an Asp in P4 is 100-fold higher than that for a Glu/Asn at this position (*16*). The structural basis for this observation was revealed recently (*43*). The *N*-terminal loop consisting of residues 176−185 of the β-subunit plays a vital role in the substrate recognition, particularly at the subsites S4 and S5. The predominant factors contributing to the binding affinity of an inhibitor are (i) a low-barrier hydrogen bond (LBHB) between the P4 Asp (in the case of **1**, **2** and **3**) and the safety catch Asp_{179}, and (ii) a cluster of hydrophobic interactions between Val_{178}, Phe_{250}, Phe_{248}, and P5-Cbz group. In contrast to the former observation (*43*), the P5-Cbz group is well-ordered in all of the crystal structures reported here (Figure 3b). The electron density map is well defined, and the B-factor values for the atoms of P5-Cbz are comparable to the rest of the inhibitor moiety. The P5-Cbz group is stabilized by the hydrophobic cluster formed by Val_{178}, Phe_{250}, Phe_{252}, and Lys_{229}.

To study the influence of the P4 residue on the ordering of the *N*-terminal loop and, in particular, the interaction that prevailed between the P4 aspartate and the safety catch Asp_{179}, we have determined two crystal structures of caspase-3 with suboptimal inhibitors containing an isoleucine residue in P4 (IETD) and a tripeptide (EVD) based inhibitor. Procaspase-3 exists as an inactive zymogen, and it is activated through proteolytic cleavage by the initiator caspase-8/-9 during apoptosis to separate the α- and the

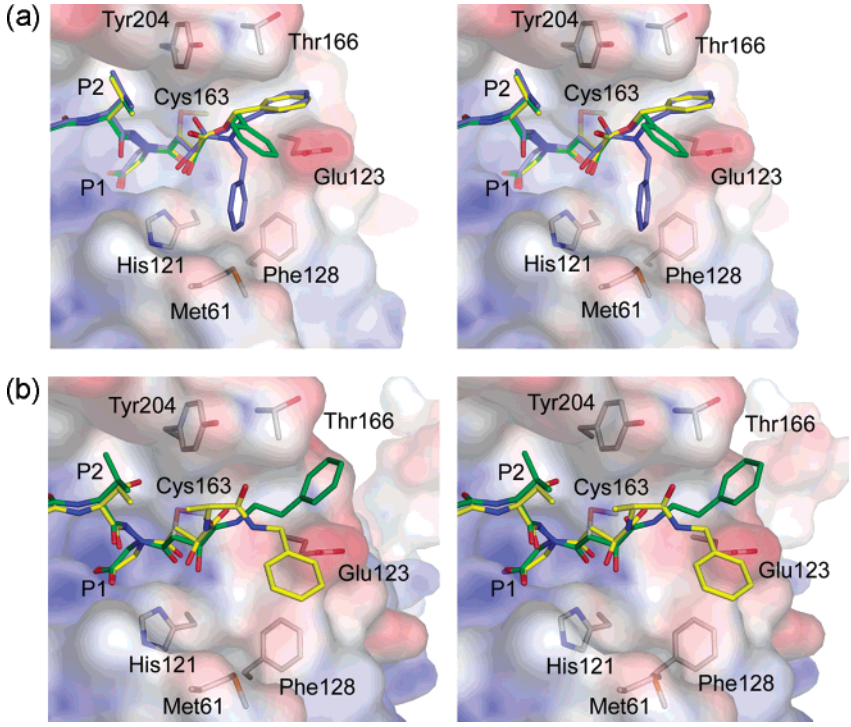

FIGURE 5: Surface representation of the active site of caspase-3. The active site and prime site residues are shown in stick representation. (a) Superposition of compounds **1** (blue), **2** (green), and compound **3** (yellow). The biphenyl derivative effectively buries the residues Tyr_{204}, Thr_{166}, Glu_{123}, Phe_{128}, and Met_{61} in the prime site. (b) Superposition of compound **4** (green) and compound **5** (yellow). The methyl group of the alanine residue of compound **5** in the prime site is stabilized through hydrophobic contacts with the P2 Thr residue.

β-subunits. The subunits then rearrange to produce an active caspase-3 molecule. Autocatalytic activation of procaspase-3 by an active caspase-3 is a way to amplify the apoptotic signal, and the cleavage occurs at Asp_{175}, located at the intersubunit linker region. The cleavage sequence (^{172}–IETD–^{175}) matches the peptide sequence of compound **5**; thus, the structure is a representation of the interactions of a substrate and the enzyme during the autocatalytic activation. In the case of compound **5**, the lower value for the second-order inactivation rate constant (k_2) emphasizes the importance of P4 Asp in comparison to the suboptimal P4 Ile residue (*23*). The P4 Ile in compound **5** topologically occupies the same place as a P4 Asp. It is stabilized through hydrophobic contacts to Trp_{206}, Trp_{214}, and Phe_{250} (Figure 6b). Large scale movements of the residues shaping the substrate binding site are observed. The most dramatic change occurs with Trp_{206}, which rotates 15° around χ1 and is thus displaced by about 1.3 Å. The movement of Trp_{206} is necessary to prevent steric clashes with the P4 Ile residue. This also influences the neighboring hydrophobic residues, such as Leu_{168}, Phe_{256}, Tyr_{204}, and Trp_{214}, all of which adapt to the needs of accommodating the suboptimal P4 Ile. These structural observations are in good agreement with the initial hypothesis concerning the reorganization of tryptophan residues during caspase-3 activation. The placement of an isoleucine residue in the S4 subsite results in the drastic decrease in affinity due to nonproductive binding. Consequently, the main chain atoms of the *N*-terminal loop of the β-subunit (residues 176–185) are displaced by about 0.5 Å in comparison to the other crystal structures in complex with compounds **1**, **2**, and **3**. No change in the side chain conformations of residues 176–185 in the *N*-terminal loop is observed. In the case of tripeptidic inhibitor **4**, the blocking group Cbz occupies the S4 pocket, and it is stabilized by hydrophobic contacts with residues Trp_{206}, Trp_{214}, and Phe_{250} (Figure 6a). An interesting feature of the structure in complex with compound **4** is that the *N*-terminal loop of the β-subunit, in particular residues 176–185, is completely disordered. No interpretable electron density for the *N*-terminal loop residues was observed. This is a consequence of the removal of both the anchor points that prevailed in the crystal structure complexes of compounds **1**, **2** and **3**.

DISCUSSION

Strategies to specifically target caspase-3 for therapeutic intervention could be fruitful in the treatment of variety of diseases. A large number of caspase/inhibitor complexes have been studied by X-ray crystallography (*12*, *35*, *36*, *42*, *44*, *45*). The caspase structures increased the understanding of their important role in apoptosis and have revealed a wide variety of binding modes and geometries. Most of the inhibitors bind to the S1–S4 subsites of the active site, whereas less is known about the binding at the S1′ subsite. In this article, we describe the structural basis for the mechanism of inhibition and the binding mode of aza-peptide epoxides by caspase-3. Analysis of the crystal structures reveals that the nucleophilic attack takes place on the C3 carbon of the epoxide ring; thus, additional substitution might be tolerated at the C2 carbon. The binding of the aza-peptides mimics the substrate-like binding in the S1–S4 subsites. In sharp contrast to clan CA cysteine proteases, the epoxide ring is protonated by the catalytic His_{121} in caspases. Our aza-peptide epoxide inhibitors demonstrate very high selectivity toward caspases. The prominent reasons for this is the design strategy of placing the epoxide moiety at the *C*-terminus of an aza aspartic acid residue resulting in the overall stabilization of the charged groups, such as the oxyanion hole, catalytic histidine, and P1 Asp of the inhibitor.

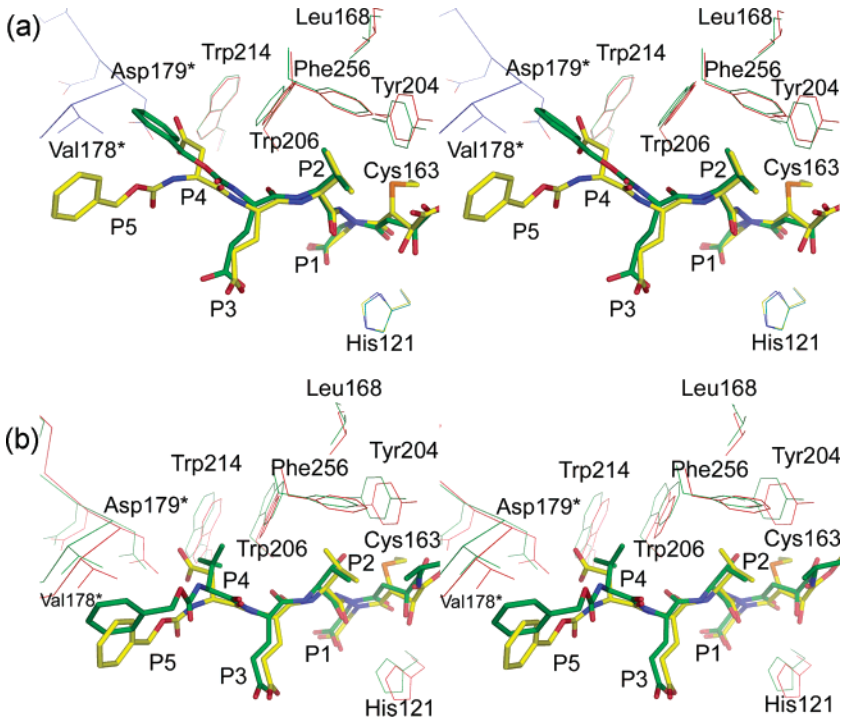

FIGURE 6: (a) Superposition of compound **4** and compound **2**. The Cbz group of compound **4** occupies the S4 binding pocket resulting in the disordering of the *N*-terminal loop (residues 176−185) of the β-subunit. (b) Superposition of compound **5** and compound **2**. The isoleucine residue in compound **5** occupies the S4 binding pocket resulting in the displacement of the *N*-terminal loop of the β-subunit by about 0.5 Å. Large scale deviations of main chain atoms as well as side chain conformations of the residues, Trp_{206}, Phe_{256}, Leu_{168}, and Trp_{214} in the selectivity loop are observed in both the crystal structures.

The other plausible reasons for selectivity might arise from the mechanistic differences between clan CA and CD cysteine proteases. The capability to recognize both D and L configurations of the substrates with similar reactivity is a unique feature of caspases (*46*). The P1 aza manipulation to form the aza-peptide results in a change in the configuration of the P1 residue from L to intermediate planar D/L geometry. The difference in geometry prevents the nucleophilic attack on the warhead group by other proteases, whereas caspases recognize compounds with this geometry as normal peptidic substrates with similar efficiency. Serine protease, like granzyme B, having a preference for aspartic acid at the P1 position, might lack the nucleophilicity required for the epoxide ring opening in an S_N2-like displacement.

Selective inhibition of a particular caspase can be achieved by exploiting the specificity at the prime site. The highly homologous executioner caspases-3 and -7 possess prime sites of slightly different size and shape. Although the prime site in caspase-7 is a deep and narrow pocket, the prime site in caspase-3 is more open and broad. We wanted to capitalize on the affinity of hydrophobic residues at the prime site to design some potent and specific inhibitors. Our inhibitors show reasonable selectivity toward caspase-3 because of the presence of the prime site constituent. The structural studies with nonideal P4 substituents revealed that the ordering of the *N*-terminal loop of the β-subunit is dictated by two key interactions: (i) the LBHB and (ii) the hydrophobic cluster discussed above. A dramatic shift occurs in the observed k2 value, if a P4 Asp is replaced by a P4 Ile, which can be explained by the large scale movements of the residues shaping the substrate binding site. The *N*-terminal loop of the β-subunit is completely disordered in the crystal structure when both key interactions are missing. This leads to insufficient charge compensation and a conformational change that decreases the binding surface, implying a drop in the binding affinity. Therefore, the S4 subsite in caspase-3 has a strong preference for an aspartic acid. In conclusion, we have highlighted the structural basis for achieving the selective inhibition of caspase-3 by utilizing the variations and subtle differences, particularly in the S4 and S1′ subsites.

ACKNOWLEDGMENT

We gratefully acknowledge Dr. Peer R. E. Mittl for fruitful discussions. We thank the Swiss Light Source, Paul Scherrer Institute, Villigen, Switzerland, for providing the synchrotron beam time and C. Schulze-Briese for his excellent support during data collection. J. Tschopp from the University of Lausanne is acknowledged for providing the caspase-3 cDNA.

SUPPORTING INFORMATION AVAILABLE

This material is available free of charge via the Internet at http://pubs.acs.org.

REFERENCES

1. Grütter, M. G. (2000) Caspases: key players in programmed cell death, *Curr. Opin. Struct. Biol. 10*, 649−655.
2. Nicholson, D. W. (1999) Caspase structure, proteolytic substrates, and function during apoptotic cell death, *Cell Death Differ. 6*, 1028−1042.
3. Gervais, F. G., Xu, D., Robertson, G. S., Vaillancourt, J. P., Zhu, Y., Huang, J., LeBlanc, A., Smith, D., Rigby, M., and Shearman, M. S. (1999) Involvement of caspases in proteolytic cleavage of Alzheimer's amyloid-β precursor protein and amyloidogenic A-β peptide formation, *Cell 97*, 395.
4. Stennicke, H. R., Deveraux, Q. L., Humke, E. W., Reed, J. C., Dixit, V. M., and Salvesen, G. S. (1999) Caspase-9 can be activated without proteolytic processing, *J. Biol. Chem. 274*, 8359−8362.
5. Stennicke, H. R., Jurgensmeier, J. M., Shin, H., Deveraux, Q., Wolf, B. B., Yang, X., Zhou, Q., Ellerby, H. M., Ellerby, L. M.,

Bredesen, D., Green, D. R., Reed, J. C., Froelich, C. J., and Salvesen, G. S. (1998) Pro-caspase-3 is a major physiologic target of caspase-8, *J. Biol. Chem. 273*, 27084−27090.
6. Gulyaeva, N. V. (2003) Non-apoptotic functions of caspase-3 in nervous tissue, *Biochemistry (Moscow) 68*, 1171−1180.
7. Gulyaeva, N. V., Kudryashov, I. E., and Kudryashova, I. V. (2003) Caspase activity is essential for long-term potentiation, *J. Neurosci. Res. 73*, 853−864.
8. Schwerk, C., and Schulze-Osthoff, K. (2003) Non-apoptotic functions of caspases in cellular proliferation and differentiation, *Biochem. Pharmacol. 66*, 1453−1458.
9. O'Brien, T. (2004) Prospects for caspase inhibitors. *Mini Rev. Med. Chem. 4*, 153−165.
10. Slee, E. A., Adrain, C., and Martin, J. S. (2001) Executioner caspase-3, -6, and -7 perform distinct, non-redundant roles during the demolition phase of apoptosis, *J. Biol. Chem. 276*, 7320−7326.
11. Thornberry, N. A., Rano, T. A., Peterson, E. P., Rasper, D. M., Timkey, T., Garcia-Calvo, M., Houtzager, V. M., Nordstrom, P. A., Roy, S., Vaillancourt, J. P., Chapman, K. T., and Nicholson, D. W. (1997) A combinatorial approach defines specificities of members of the caspase family and granzyme B. Functional relationships established for key mediators of apoptosis, *J. Biol. Chem. 272*, 17907−17911.
12. Fuentes-Prior, P., and Salvesen, G. S. (2004) The protein structures that shape caspase activity, specificity, activation and inhibition, *Biochem. J. 384*, 201−232.
13. Becker, J. W. (2004) Reducing the peptidyl features of caspase-3 inhibitors: a structural analysis, *J. Med. Chem. 47*, 2466−74.
14. Goode, D. R., Sharma, A. K., and Hergenrother, P. J. (2005) Using peptidic inhibitors to systematically probe the S1′ site of caspase-3 and caspase-7, *Org. Lett. 7*, 3529−3532.
15. Petrassi, H. M., Williams, J. A., Li, J., Tumanut, C., Ek, J., Nakai, T., Masick, B., Backes, B. J., and Harris, J. L. (2005) A strategy to profile prime and nonprime proteolytic substrate specificity, *Bioorg. Med. Chem. Lett. 15*, 3162.
16. Stennicke, H. R., Renatus, M., Meldal, M., and Salvesen, G. S. (2000) Internally quenched fluorescent peptide substrates disclose the subsite preferences of human caspases 1, 3, 6, 7 and 8, *Biochem. J. 350*, 563−568.
17. Gray, J., Haran, M. M., Schneider, K., Vesce, S., Ray, A. M., Owen, D., White, I. R., Cutler, P., and Davis, J. B. (2001) Evidence that inhibition of cathepsin-B contributes to the neuroprotective properties of caspase inhibitor Tyr-Val-Ala-Asp-chloromethyl ketone, *J. Biol. Chem. 276*, 32750−32755.
18. Rozman-Pungercar, J., Kopitar-Jerala, N., Bogyo, M., Turk, D., Vasiljeva, O., Stefe, I., Vandenabeele, P., Bromme, D., Puizdar, V., Fonovic, M., Trstenjak-Prebanda, M., Dolenc, I., Turk, V., and Turk, B. (2003) Inhibition of papain-like cysteine proteases and legumain by caspase-specific inhibitors: when reaction mechanism is more important than specificity, *Cell Death Differ. 10*, 881−888.
19. Schotte, P., Declercq, W., Van Huffel, S., Vandenabeele, P., and Beyaert, R. (1999) Non-specific effects of methyl ketone peptide inhibitors of caspases, *FEBS Lett. 442*, 117.
20. Schotte, P., Van Criekinge, W., Van de Craen, M., Van Loo, G., Desmedt, M., Grooten, J., Cornelissen, M., De Ridder, L., Vandekerckhove, J., and Fiers, W. (1998) Cathepsin B-mediated activation of the proinflammatory caspase-11, *Biochem. Biophys. Res. Commun. 251*, 379.
21. Asgian, J. L., James, K. E., Li, Z. Z., Carter, W., Barrett, A. J., Mikolajczyk, J., Salvesen, G. S., and Powers, J. C. (2002) Aza-peptide epoxides: a new class of inhibitors selective for clan CD cysteine proteases, *J. Med. Chem. 45*, 4958−4960.
22. Ekici, O. D., Gotz, M. G., James, K. E., Li, Z. Z., Rukamp, B. J., Asgian, J. L., Caffrey, C. R., Hansell, E., Dvorak, J., McKerrow, J. H., Potempa, J., Travis, J., Mikolajczyk, J., Salvesen, G. S., and Powers, J. C. (2004) Aza-peptide Michael acceptors: a new class of inhibitors specific for caspases and other clan CD cysteine proteases, *J. Med. Chem. 47*, 1889−1892.
23. James, K. E., Asgian, J. L., Li, Z. Z., Ekici, O. D., Rubin, J. R., Mikolajczyk, J., Salvesen, G. S., and Powers, J. C. (2004) Design, synthesis, and evaluation of aza-peptide epoxides as selective and potent inhibitors of caspases-1, -3, -6, and -8, *J. Med. Chem. 47*, 1553−1574.
24. Evans, P. R. (1992) Data reduction. Proceedings of the CCP4 study weekend on data collection and processing.
25. Leslie, A. G. W. (1992) SCALA. *Joint CCP4/ESF-EACMB Newsletter on Protein Crystallography 26*.
26. Kabsch, W. (1988) Automatic indexing of rotation diffraction patterns, *J. Appl. Crystallogr. 21*, 67−72.
27. Brunger, A. T., Adams, P. D., Clore, G. M., DeLano, W. L., Gros, P., Grosse-Kunstleve, R. W., Jiang, J. S., Kuszewski, J., Nilges, M., Pannu, N. S., Read, R. J., Rice, L. M., Simonson, T., and Warren, G. L. (1998) Crystallography & NMR system: A new software suite for macromolecular structure determination, *Acta Crystallogr., Sect. D 54*, 905−921.
28. Jones, T. A., Zou, J. Y., Cowan, S. W., and Kjeldgaard. (1991) Improved methods for building protein models in electron density maps and the location of errors in these models, *Acta Crystallogr., Sect. A 47*, 110−119.
29. Powers, J. C., Asgian, J. L., Ekici, O. D., and James, K. E. (2002) Irreversible inhibitors of serine, cysteine, and threonine proteases, *Chem. Rev. 102*, 4639−4750.
30. Bajusz, S., Fauszt, I., Nemeth, K., Barabas, E., Juhasz, A., Patthy, M., and Bauer, P. I. (1999) Peptidyl beta-homo-aspartals (3-amino-4-carboxybutyraldehydes): new specific inhibitors of caspases, *Biopolymers 51*, 109−118.
31. Schirmeister, T., and Klockow, A. (2003) Cysteine protease inhibitors containing small rings, *Mini Rev. Med. Chem. 3*, 589.
32. Gupton, B. F., Carroll, D. L., Tuhy, P. M., Kam, C. M., and Powers, J. C. (1984) Reaction of azapeptides with chymotrypsin-like enzymes. New inhibitors and active site titrants for chymotrypsin A alpha, subtilisin BPN′, subtilisin Carlsberg, and human leukocyte cathepsin G, *J. Biol. Chem. 259*, 4279−4287.
33. Otto, H. H., and Schirmeister, T. (1997) Cysteine proteases and their inhibitors, *Chem. Rev. 97*, 133−172.
34. Varughese, K. I., Ahmed, F. R., Carey, P. R., Hasnain, S., Huber, C. P., and Storer, A. C. (1989) Crystal structure of a papain-E-64 complex, *Biochemistry 28*, 1330−1332.
35. Mittl, P. R., Di Marco, S., Krebs, J. F., Bai, X., Karanewsky, D. S., Priestle, J. P., Tomaselli, K. J., and Grütter, M. G. (1997) Structure of recombinant human CPP32 in complex with the tetrapeptide acetyl-Asp-Val-Ala-Asp fluoromethyl ketone, *J. Biol. Chem. 272*, 6539−6547.
36. Rotonda, J., Nicholson, D. W., Fazil, K. M., Gallant, M., Gareau, Y., Labelle, M., Peterson, E. P., Rasper, D. M., Ruel, R., Vaillancourt, J. P., Thornberry, N. A., and Becker, J. W. (1996) The three-dimensional structure of apopain/CPP32, a key mediator of apoptosis, *Nat. Struct. Biol. 3*, 619−625.
37. Anamarija Zega, U. U. (2002) Azapeptides, *Acta Chim. Slov. 49*, 649−662.
38. Gante, J. (1989) Azapeptides, *Synthesis*, 405−413.
39. Thormann, M., and Hofmann, H. J. (1999) Conformational properties of azapeptides, *J. Mol. Struct.* (*Theochem.*) *469*, 63−76.
40. Hartmut Niedrich, and Christa Oehme. (1972) Hydrazinverbindungen als heterobestandteile in peptiden. XV. Synthese von eledoisin-octapeptiden mit den carbazylresten azaglycin und α-azaasparagin statt glycin und asparagin, *J. Prakt. Chem. 314*, 759−768.
41. Mullican, M. D., Lauffer, D. J., Gillespie, R. J., Matharu, S. S., Kay, D., Porritt, G. M., Evans, P. L., Golec, J. M. C., and Murcko, M. A. (1994) The synthesis and evaluation of peptidyl aspartyl aldehydes as inhibitors of ICE, *Bioorg. Med. Chem. Lett. 4*, 2359.
42. Blanchard, H., Kodandapani, L., Mittl, P. R., Marco, S. D., Krebs, J. F., Wu, J. C., Tomaselli, K. J., and Grütter, M. G. (1999) The three-dimensional structure of caspase-8: an initiator enzyme in apoptosis, *Structure 7*, 1125−1133.
43. Ganesan, R., Mittl, P. R., Jelakovic, S., and Grütter, M. G. (2006) Extended substrate recognition in caspase-3 revealed by high-resolution X-ray structure analysis, *J. Mol. Biol. 359*(5), 1378−1388.
44. Watt, W., Koeplinger, K. A., Mildner, A. M., Heinrikson, R. L., Tomasselli, A. G., and Watenpaugh, K. D. (1999) The atomic-resolution structure of human caspase-8, a key activator of apoptosis, *Structure 7*, 1135−1143.
45. Wilson, K. P., Black, J. A., Thomson, J. A., Kim, E. E., Griffith, J. P., Navia, M. A., Murcko, M. A., Chambers, S. P., Aldape, R. A., Raybuck, S. A., and et al. (1994) Structure and mechanism of interleukin-1 beta converting enzyme, *Nature 370*, 270−275.
46. Prasad, C. V. C., Prouty, C. P., Hoyer, D., Ross, T. M., Salvino, J. M., Awad, M., Graybill, T. L., Schmidt, S. J., Kelly Osifo, I., and Dolle, R. E. (1995) Structural and stereochemical requirements of time-dependent inactivators of the interleukin-1[beta] converting enzyme, *Bioorg. Med. Chem. Lett. 5*, 315.

BI060364P